



# Auto-thermal combustion of CH<sub>4</sub> and CH<sub>4</sub>–H<sub>2</sub> mixtures over bi-functional Pt–LaMnO<sub>3</sub> catalytic honeycomb

P.S. Barbato<sup>a</sup>, G. Landi<sup>b</sup>, R. Pirone<sup>b,\*</sup>, G. Russo<sup>a</sup>, A. Scarpa<sup>a</sup>

<sup>a</sup> Department of Chemical Engineering, University of Naples Federico II, P.le Tecchio 80, 80125 Naples, Italy

<sup>b</sup> Istituto di Ricerche sulla Combustione, CNR, P.le Tecchio 80, 80125 Naples, Italy

## ARTICLE INFO

### Article history:

Available online 8 August 2009

### Keywords:

Combustion

CH<sub>4</sub>–H<sub>2</sub>

Pt–LaMnO<sub>3</sub>

## ABSTRACT

The range of conditions of stable operation of a catalytic honeycomb-type monolith has been investigated for the combustion of methane. Catalyst is constituted by a Pt–LaMnO<sub>3</sub> active phase supported on a γ-Al<sub>2</sub>O<sub>3</sub> washcoat deposited onto the internal channels of 900 cpsi commercial cordierite monolith via a dip-coating technique. The auto-thermal operation of the catalytic reactor is assured provided a certain amount of heat is supplied with an external furnace. The ignition of the CH<sub>4</sub>/O<sub>2</sub> mixture occurs at a defined pre-heating temperature that is a decreasing function of methane concentration and approximately constant with the total flow rate. Once the system is ignited, pre-heating temperature can be lowered also of 150–250 °C, depending on the flow rate, before quenching occurs. System quenching occurs due to extinction at lower investigated flow rates, or to blowout at the highest flow rate investigated. Such ignition/quenching temperatures have been also evaluated when an energetically equivalent CH<sub>4</sub>–H<sub>2</sub> is used as fuel, recognizing that only ignition takes a large and significant advantage by the presence of hydrogen, since quenching occurs at the same pre-heating temperature whatever the fuel composition, being it a phenomenon basically controlled by energy balance with surroundings (heat losses). On the other hand, by partially substituting of fraction of methane with hydrogen the ignition temperature can be lowered of an amount that is higher the higher the flow rate.

© 2009 Elsevier B.V. All rights reserved.

## 1. Introduction

Catalytic combustion has been widely studied as an alternative and environmental friendly route to produce energy from fossil fuel, which will remain the basic power source for next decades. Moreover, the use of a catalyst allows oxidizing fuels also outside their corresponding flammability limits, with consequent advantages on safety and on the possibility of recover energy by poor or diluted mixtures (as for example, exhausts or stacks of chemical/industrial processes). In this context, structured catalytic reactors seem to be the unavoidable choice for the reactor configuration, due to their specific features (low pressure drops, high resistance to mechanical and thermal shocks, high geometrical surface). Honeycomb-type catalytic monoliths have been widely studied as alternative systems to traditional combustion chambers for gas turbine applications and radiant heaters for both domestic and industrial applications [1]. Moreover, catalytic combustion on micro-structured reactors has been recently proposed as the best

route for the development of micro-generators of energy for portable applications [2] and of micro-fuel processors [3] where catalytic combustion produces the heat necessary to drive endothermic reactions.

However, commercialization of microcombustors was still limited due to the drawbacks related to constrained operation windows (especially in terms of operating temperature), catalyst instability and high costs of active phases essentially based on expensive noble metals [1].

Up to date, the most investigated combustion catalysts are in fact supported noble metals, in particular Pd for CH<sub>4</sub> [4] and Pt for light hydrocarbons and hydrogen [5], although they do not exhibit the stability properties at high temperatures (≥800 °C) required for practical applications [4]. Less attention has been devoted to methane combustion at micro-scales; due to its lower activity with respect to other hydrocarbons, catalytic CH<sub>4</sub> burners must operate at temperatures higher than 700 °C, strongly supporting the use of transition metal mixed oxides instead of more volatile and unstable noble metals [6].

In fact, due to their potentially higher thermal stability, non-noble metal based catalysts are very studied for combustion applications, both for the purpose of methane abatement in

\* Corresponding author.

E-mail address: [pirone@irc.cnr.it](mailto:pirone@irc.cnr.it) (R. Pirone).

exhaust gases and to develop novel processes of energy production [7–10], but very rarely such investigations have been brought close to the level of practical applications.

Mixed oxides with perovskite structure seem to be the most active systems among non-noble metal based catalysts for deep oxidation reactions, major limitation being related to their low surface area. One possible solution is the dispersion of perovskites over high porous and possibly high heat-resistant supports [6,11].

On the other hand, very few are the studies on the preparation of structured catalysts based on transition metals [7,12,13], and even less are the contributions that investigate the behavior of the system in auto-thermal, if not quasi-adiabatic, conditions, when transport phenomena, reaction rate, heat losses and chemico-physical properties of the material (heat conductivity, heat capacity, expansion coefficient, etc.) concur to give to affect the range of stable operation conditions [12,14]. Moreover, at high temperatures (around 1000 °C or more) also radiation plays a relevant role in determining the reactor behavior, its thermal profiles and ignition/extinction dynamics [32]. However, such conditions are very representative of microcombustors operation. In particular, the presence of heat losses at micro-scale is unavoidable due to the high value of surface-to-volume ratio, and is often desired since a fraction of heat must be transferred to the conversion system in micro-generators, so severely affecting the stability map of the entire micro-burner.

Actually, it has been reported that auto-thermal combustion in microcombustors is stable in a narrow operating window because of the occurrence of two quenching modes, extinction and blowout, associated to a drop in temperature and conversion [15–17] due to different causes. In the extinction mode, stability is lost due to a too large heat loss (towards surroundings) compared to the thermal power provided via combustion. In the blowout mode, quenching occurs because of a too large flow rate, resulting in incomplete fuel conversion for both insufficient residence time and a considerable shift of the reaction front downstream, due to insufficient cold feed gas pre-heating.

Moreover, methane reactivity should result increased by the addition of hydrogen [18], even if some controversial result has been reported for noble metal based catalysts: Demoulin et al. [19,20] reported that hydrogen can either promote or inhibit the efficiency of the Pd/ $\gamma$ -Al<sub>2</sub>O<sub>3</sub> catalyst, depending on H<sub>2</sub> concentration, since it can modify catalyst properties.

In effect, the use of CH<sub>4</sub>–H<sub>2</sub> mixtures as fuel could represent an efficient way for hydrogen to penetrate the energy market, as well as a tool to promote higher combustion efficiency and lower environmental impact. We recently proposed bi-functional catalysts based on Pt and LaMnO<sub>3</sub> for microcombustion of propane [21] and methane [22], showing that it is the best compromised catalyst to burn CH<sub>4</sub>–H<sub>2</sub> mixtures, since Pt is very active for hydrogen and perovskite is more active for methane. We also showed that under controlled temperature, isothermal conditions and very diluted fuel–oxygen mixtures, the thermal dissociation of H<sub>2</sub> promotes the formation of radicals that attacks CH<sub>4</sub> as well as H<sub>2</sub>, so allowing methane oxidation in a range of relatively low temperature.

However, the concept of join the properties of noble metals with those of perovskite is arising in recent times and many studies have been published on this subject [23–27]. The basic idea driving this approach is to obtain very active catalysts at low temperature (due to the noble metal properties) but also stable and active at relatively high temperature (thanks to perovskite), trying to keep the noble metal content to very low values in the meanwhile, in order to limit the catalyst overall cost. For methane combustion, the most investigated systems are Pd-based catalysts with the noble metal inserted into LaMnO<sub>3</sub> [23–25] or Pd/LaCoO<sub>3</sub> [26,27] structures, the former providing the best performance.

In this work the behavior of such a Pt–LaMnO<sub>3</sub> catalyst able to operate in a stable way at around 1000 °C has been evaluated in the combustion of CH<sub>4</sub>, with and without H<sub>2</sub> addition, under auto-thermal conditions. Commercial substrate coated with a thin layer of catalyst have been investigated by varying the GHSV, the reacting mixture composition, the pre-heating temperature and analyzing the stability of the catalytic combustion. Aim of our study is to demonstrate the effectiveness of a much cheaper catalyst under real conditions, characterized by higher temperature and significant fuel concentrations and to analyze the conditions of stable operation of the reactor, and the possible role of H<sub>2</sub> addition in the fuel to enlarge the operability window.

## 2. Experimental

### 2.1. Monolith preparation

Structured catalysts, constituted by Pt–LaMnO<sub>3</sub>/ $\gamma$ -Al<sub>2</sub>O<sub>3</sub>, have been prepared starting from commercial cordierite monoliths, provided by NGK (900 cpsi); the substrates were previously cut in the shape of disks (12 mm long and 17 mm wide) and subsequently coated with a thick La<sub>2</sub>O<sub>3</sub>-stabilized  $\gamma$ -Al<sub>2</sub>O<sub>3</sub> layer by using a dip-coating procedure and calcined in air at 800 °C [6]. Pt and perovskite precursors were deposited on the stabilized alumina washcoat through impregnation with an aqueous solution of La(NO<sub>3</sub>)<sub>3</sub>·6H<sub>2</sub>O (Aldrich, >99.99%), (CH<sub>3</sub>CO<sub>2</sub>)<sub>2</sub>Mn·4H<sub>2</sub>O (Aldrich, >99%) and H<sub>2</sub>PtCl<sub>6</sub> (Sigma, 8 wt% solution). The samples were dried in MW oven and in stove at 120 °C and calcined at 800 °C for 3 h under flowing air. The process was repeated 10 times in order to achieve the target loading (~20 wt% perovskite and 1 wt% Pt with respect to the active washcoat layer, monolithic substrate excluded). The adopted procedure allowed us to deposit about 1.1 g of catalyst onto the substrates.

Catalytic monoliths before being tested are aged by exposure to combustion environment, at  $T$  = 800–900 °C and at a carbon dioxide and water concentrations ranging within 6–10 vol%, for about 5–10 h.

Chemical composition of the fresh and aged catalyst has been measured by means of inductively coupled plasma (ICP) analysis, performed on an Agilent 7500 ICP-MS instrument.

### 2.2. Catalytic tests

A quartz lab-scale reactor has been set up for the study of auto-thermal combustion on monolith catalysts. A reactor drawing is reported in Fig. 1. It consists of a cylindrical quartz tube whose external and internal diameters are respectively 25.4 and 23.9 mm. The monolith catalyst is inserted inside the tube and placed between two ceramic foams (25 mm long) acting as thermal shields. In order to avoid bypass of the reacting flow, monolith and foams are wrapped in a thin alumina blanket before being inserted in the quartz tube.

Three K-type thermocouples are inserted inside the catalyst monolith (i.e. inside one central channel), thus providing the measurement of temperature profiles; specifically, temperature is detected close to the inlet (approximately 3 mm far from the inlet), at the middle and close to the end (approximately 3 mm far from the outlet) of the catalyst. The thermocouples in the catalytic honeycomb had its tip (0.5 mm) placed in close contact with the solid wall and the gas flow in the measuring channel was strongly reduced due to the presence of the thermocouples themselves: therefore the temperatures reading in the honeycomb catalyst are believed to be more indicative of the surface temperature, although, in general, it is a weighted-average with gas temperature.

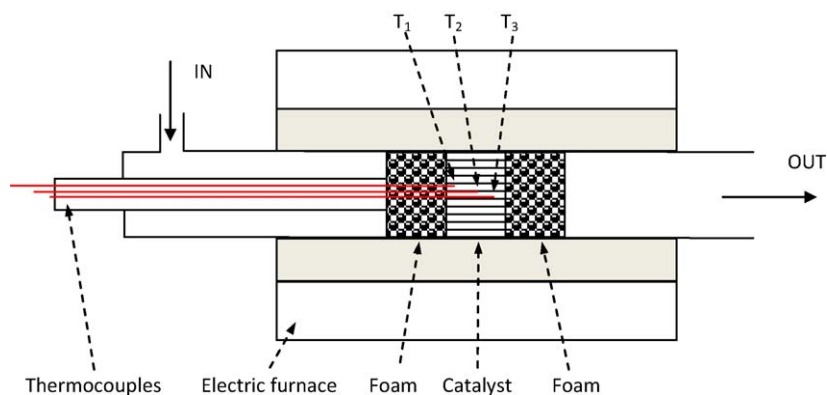


**Fig. 1.** Schematic drawing of the catalytic reactor with indications of flow path and thermocouple placement. Shape factors have not been respected in order to enlighten the relative positions of the thermocouples.

High purity gas cylinders have been used in order to supply methane (99.995% purity), oxygen (99.7%) and nitrogen (99.998%), while hydrogen have been produced by means of a hydrogen generator (HG2400, Claind). Gas flow rates are controlled through mass flow controllers (MFC 5850E, Brooks), providing a total flow rate between 40 and 140 slph (standard liters per hour). An ice bath based condenser and a  $\text{CaCl}_2$  trap are used in order to dry the gaseous flow downstream to the reactor; the dried flow is analyzed in a Fisher-Rosemount NGA2000 continuous analyzer to continuously measure  $\text{CH}_4$ ,  $\text{CO}$ ,  $\text{CO}_2$ ,  $\text{H}_2$  and  $\text{O}_2$  concentrations. Selectivity to  $\text{CO}$  or  $\text{CO}_2$  will not be reported in the following, because no carbon monoxide has been detected in all the performed combustion tests (the sensibility of the analyser is around 5 ppm).

Fuel mixtures are ignited by means of electric tubular furnaces (Lenton), provided with a PID-type controller and working at a maximum temperature of  $1200^\circ\text{C}$ . Experiments were carried out under pseudo-auto-thermal conditions, so meaning that, provided a certain amount of heat is furnished from outside, the heat generated by the reaction should be high enough to guarantee the self-sustainability of the combustion process. Actually, in most cases the heat losses are too high to allow thermal auto-sustainability with sole reaction heat; external heat is supplied by maintaining the entire system at a controlled temperature with the electric furnace. Such a controlled temperature of the entire external system is here defined the “pre-heating temperature”, since it can be assumed as the temperature of the entering gas.

With such an experimental approach, two are the properties of the system that have been evaluated: the light-off and the quenching temperature, that have been measured with varying inlet fuel compositions and total flow rate, as reported in Table 1. For safety issues, fuel composition was always outside flamm-

ability region, keeping  $\text{CH}_4$  and  $\text{H}_2$  inlet concentrations below LFL and  $\text{O}_2$  at 10 vol%, a value sufficiently high to be in excess with respect the total combustion stoichiometry but not higher than MOC.

As it can be evident in Table 1, four different fuel composition are chosen.  $\text{CH}_4$ – $\text{H}_2$  mixture, Mix3, is characterized by the same overall heating value of Mix1 and a  $\text{H}_2/\text{CH}_4$  ratio of 0.95 corresponding to a substitution of methane with hydrogen of 49% as regards the molar content or 22% considering the energetic content of  $\text{H}_2$  with respect to the overall mixture. Mix4 has been prepared with the same hydrogen content as Mix3 and by replacing  $\text{CH}_4$  with  $\text{N}_2$ . Such a fuel has been considered as a reference of the thermal power supplied by hydrogen in  $\text{CH}_4$ – $\text{H}_2$  combustion. Finally, total flow rate varied from 40 to 140 slph corresponding to an input power in 2–50 W range.

In the following the minimum ignition temperature (MIT) and quenching temperature (QT) will be reported as a function of the pre-heating temperature. MIT is here defined as the gas temperature at which light-off occurs at the minimum pre-heating, while QT corresponds to the minimum value of entering gas temperature that allows stable combustion.

### 3. Results

ICP analysis performed over both fresh and aged catalyst shows that the Pt content indicates a reasonable agreement between the expected and the theoretical noble metal loading, suggesting that the preparation method guarantees the desired catalyst composition and indicate good anchoring of the catalytic layer on the cordierite substrate and no measurable Pt volatilization.

#### 3.1. Methane ignition and quenching

In order to study the range of conditions of stable operation for the catalytic combustion over the  $\text{Pt-LaMnO}_3$  monolith, we have defined two characterizing properties: the minimum ignition temperature and the quenching temperature for a certain fuel–oxygen mixture, that have been measured according to a specific experimental procedure. Specifically, the system is heated (reactor, catalyst, gas feeding tubes) in inert atmosphere ( $\text{N}_2$ ) up to a specific set-point furnace temperature. Then the reactants mixture is fed to the reactor and temperature profile inside the catalyst as well as fuel conversion are continuously measured. If conversion does not go to about 100% and temperature is not drastically increased, temperature set-point of the external electric furnace is increased with a step of  $5^\circ\text{C}$  (under inert atmosphere) and the procedure is repeated till fuel ignites and reaches 100% steady state combustion after an often long transient phase. Under these conditions, MIT is

**Table 1**  
Characteristics of fuel mixtures.

	Fuel			
	$\text{CH}_4$		$\text{CH}_4$ – $\text{H}_2$	$\text{H}_2$
	Mix1	Mix2	Mix3	Mix4
$\text{H}_2$ (%)	–	–	2.1	2.1
$\text{CH}_4$ (%)	2.8	3.8	2.2	–
$\text{O}_2$ (%)	10.0	10.0	10.0	10.0
$\text{N}_2$ (%)	87.2	86.2	85.7	87.9
Equivalence ratio ( $\Phi$ )	0.56	0.76	0.54	0.1
Heating value ( $\text{kJ Nl}^{-1}$ )	0.9	1.2	0.9	0.2
Thermal power (W)	10–35	13–47	10–35	2–8

$Q_{\text{TOT}} = 40$ – $140$  slph

found through temperature measurements made with thermocouples inserted in the monolith (that are in general different from the actual furnace temperature). After fuel mixture ignition, steady states of methane combustion are measured by decreasing furnace set-point temperature until to reach a value of pre-heating temperature that is insufficient to sustain an ignited state of the system, that is here defined as the quenching point QT.

As regards the ignition phenomena the temperature considered is the exit one, which is the highest in the absence of the reaction (under inert flux); on the contrary the quenching temperature is the entrance one, which corresponds to about the pre-heating temperature of the gas.

In Fig. 2, such a procedure is summarized and presented for the combustion of Mix1 at a total flow rate of 80 slph, by reporting the steady state values of methane conversion as a function of the pre-heating temperature applied. The figure shows a S-shape curve with two different branches, related to multiple steady states, typical of high exothermic reactions (e.g. [30]). As reported in Fig. 2, light-off occurs at about 530 °C, which corresponds to MIT according to our notations, while quenching takes place when pre-heating temperature is below 330 °C.

Temperature profiles (Fig. 2b) show the presence of a maximum placed in the middle part of the reactor, where the reaction front is anchored. The degree of non-adiabaticity can be related to the difference between measured and adiabatic temperatures and is due to heat losses mostly occurring in the second half of the reactor (post-combustion zone). This phenomenon is typical of micro-reactors [5] and has been successfully modeled on Pt-based catalytic microtubes [31]. The temperature and CH<sub>4</sub> concentration profiles shown by these Authors indicated that the reaction front is close to the entrance and influenced by the occurrence of gas phase reaction, while the second part of the reactor works as an heat exchanger. In our case, it seems that the reaction front is more

likely anchored in the middle zone; several concurrent reasons can explain this difference. In [31], methane inlet concentration is inside the flammability limits, while our experiments are performed below LFL with probable different reaction kinetics (the combustion rate is lower); for this reason as well as for the different heat exchange with the surroundings, i.e. different heat losses, the temperature profiles, even representing the same shape, show a maximum characterized by a different value and position.

By decreasing the pre-heating temperature a general decrease in the temperature level is observed as a consequence of the lower adiabatic temperature, but also due to the small, even if significant decrease of methane conversion. However, the impact on the three measured temperatures is different,  $T_1$  showing the most and  $T_3$  the less significant decreases. This behavior is due to a shift of the reaction front downstream and, as a consequence, an extension of pre-heating zone and a reduction of the post-combustion zone. This typically occurs on perovskite catalysts, as our research group has been previously reported [12]. The effect of the above phenomena is the reduction of the reactor section available for fuel activation (because of the too low temperature of a large entrance part), leading to incomplete conversion; thus, the generated power decreases and heat losses become more and more significant in the energy balance, causing a decrease of surface temperature and activity down to values incompatible with self-sustained operation (Fig. 2a).

In Fig. 3 it is reported the transient of the ignition at MIT measured feeding Mix1 at a total flow rate of 80 slph, according to the above reported procedure. When methane is added to the gas (Zone 2) a sudden temperature increase is noted due to about 10% methane conversion. Subsequently, temperature and conversion increases in a continuous but slow way with time on stream (Zone 3) due to heat accumulation and progressive rise of reaction rate. After about 75 min combustion “run-away” occurs, methane conversion reaching about 100% without any measurable carbon monoxide production. It must be underlined that we hypothesize that ignition depends on kinetics, as also stated in [12,32], as

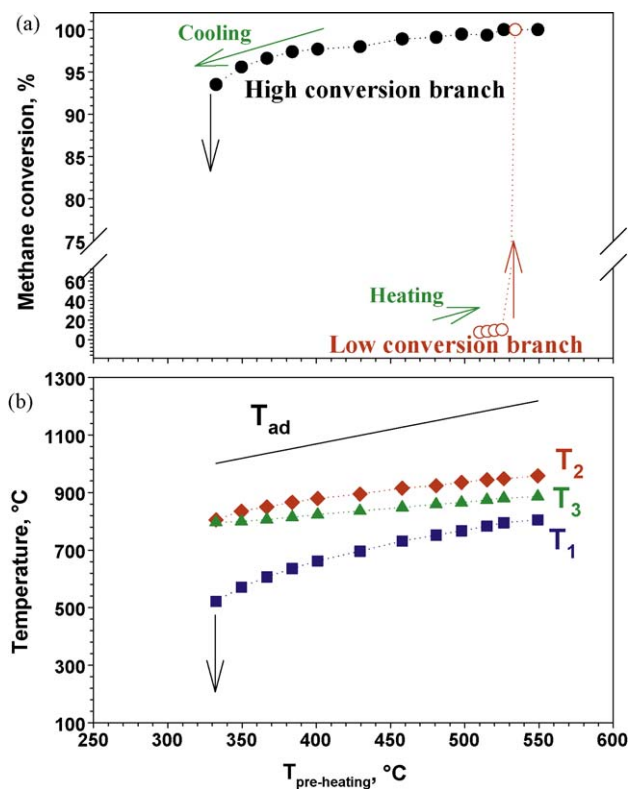


**Fig. 2.** Stability limits of CH<sub>4</sub> combustion; QT for Mix1 at  $Q_{TOT} = 80$  slph as a function of  $T_{pre-heating}$ . (a) CH<sub>4</sub> conversion: high (●) and low (○) conversion branches. (b) Temperature in the high conversion branch and theoretical adiabatic temperature ( $T_{ad}$ ).

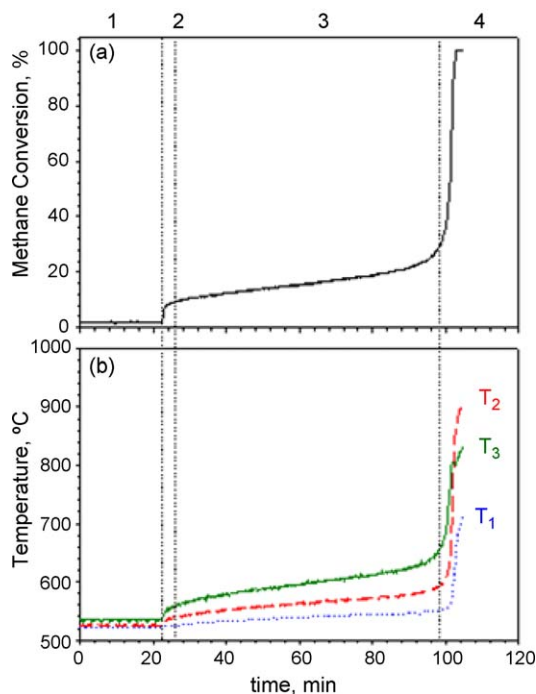


**Fig. 3.** CH<sub>4</sub> MIT evaluation. Experimental conditions:  $Q_{TOT} = 80$  slph; Mix1. Section 1: thermal profile for an O<sub>2</sub>–N<sub>2</sub> mixture. Sections 2–4: CH<sub>4</sub> is fed to the reactor: fuel light-off. (a) CH<sub>4</sub> conversion; (b) thermal profile inside the monolith ( $T_1$ : dotted line;  $T_2$ : dashed line;  $T_3$ : solid line).



suggested by the typical low conversion values obtained before ignition and by the ignition delay detected increasing the flow rate. This is a characteristic low temperature behavior, reported, for example, on Rh based catalysts under fuel-rich conditions [33,34]. As previously described [32], methane ignition depends on the surface ratio between  $\text{CH}_4$  and  $\text{O}_2$ , i.e. on the adsorption/desorption equilibria of these two species, and, as a consequence, on the catalyst type.

The total selectivity to  $\text{CO}_2$  of the process points out that methane is converted on the heterogeneous phase, being CO one main product of homogeneous combustion in this range of operating conditions [1]. Moreover, the potential thermal power is completely developed and, as a consequence, system temperature strongly raises, even if clearly it does not reach the value expected in the case of adiabatic temperature raise (heat losses play a relevant role).

The analysis of the three temperature values that have been monitored shows that the ignition takes place at the exit of the monolith where the temperature is higher. In fact, Fig. 3b clearly shows that a temperature “jump” firstly occurs for  $T_3$  and then for  $T_2$  and  $T_1$ . Differently from the thermal profile measured in Zones 2 and 3, in correspondence with the fuel ignition, maximum temperature shifts from the exit to the center of the reactor, suggesting that a different mechanism rule the thermal profile after the ignition, basically determined by the heat losses. Actually, a temperature wave travelling from the exit to the inlet of the reactor is thus observed pointing out the reaction front propagation backwards, by means of catalyst conductivity and internal radiation between channel surfaces [12]. A similar ignition behavior has been observed by Cimino et al. on perovskite catalysts [12] and also under fuel-rich conditions on Rh catalysts [33,34]. However, temperature decreases with the axial coordinate due to the heat losses in the absence of developing reaction heat, since it is very likely that methane has been totally converted very close to the entrance of the monolithic catalyst, as already reported [12,31,35].

Temperature and methane conversion measurements during reactor quenching at a pre-heating temperature slightly lower than QT at 80 slph are reported for Mix1 as a function of time in Fig. 4. The inlet and the centered temperatures simultaneously start to decrease while  $T_3$  slightly increases till to exceed  $T_2$ , thus showing a typical quenching behavior via extinction. Even if at elevated temperatures and high conversion degrees mass transfer probably is the controlling process, extinction phenomena in the presence of a catalyst seem to be related to chemical factors [36]; as a matter of fact, Cimino et al. [12] reproduced catalyst quenching applying a kinetic model that takes into account heat losses too.

Fig. 5 shows the temperatures measured inside the reactor during the high conversion branch at different flow rates. As usually, the reported arrows point out the quenching temperature observed and the window of stable combustion at the different operating conditions. It is shown that the quenching temperature progressively decreases with increasing flow rate from 40 to 120 slph, thus extending the limits of stable combustion. On the contrary, it starts to decrease further increasing flow rate from 120 to 140 slph, indicating a different behavior. In particular,  $T_1$  increases by increasing the flow rate from 40 to 80 slph, while is practically unchanged varying the gas flow from 80 to 140 slph. On the other hand,  $T_2$  increases in a larger flow rate range; specifically,  $T_2$  progressively increases by increasing flow rate up to 120 slph while does not vary any more for a further increase to 140 slph. Finally,  $T_3$  increases in all the investigated flow rate range.

By increasing the flow rate a dual effect is expected on combustion stability. In particular, having kept the fuel composition constant, the power developed by the combustion (at complete fuel conversion) linearly increases with the flow rate.

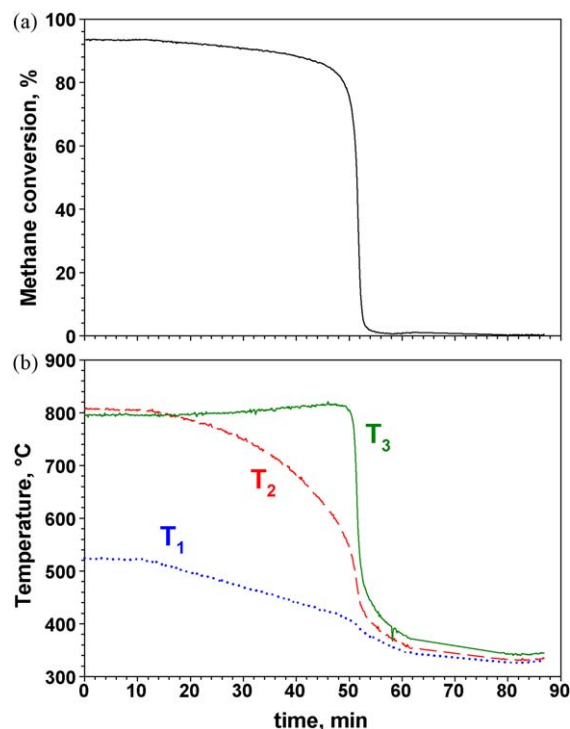
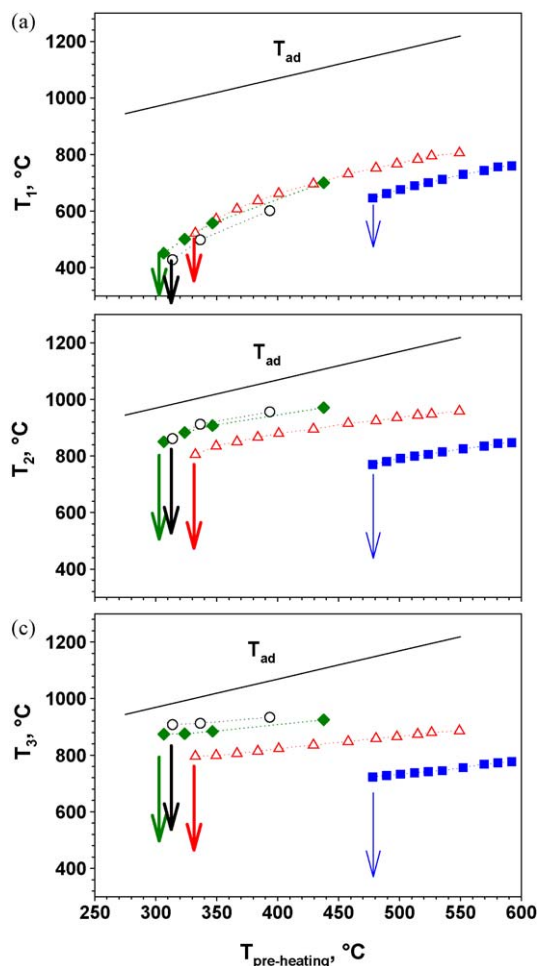


Fig. 4.  $\text{CH}_4$  quenching transient. Experimental conditions:  $Q_{\text{TOT}} = 80$  slph; Mix1. (a)  $\text{CH}_4$  conversion. (b) Temperature measurements.

At the steady state under non adiabatic conditions, the adiabaticity degree increases with flow rate at complete fuel conversion, as reported elsewhere [28], because heat losses are a fraction less and less important and catalyst temperature tends to approach the adiabatic value. Nevertheless, an increase in the flow rate brings about a decrease in the contact time and, as a consequence, a possible worsening of fuel conversion, if contact time becomes insufficient. Generally, at increased flow rate a shift of peak temperature downstream is detected [31]. These considerations suggest a tradeoff behavior regarding the total flow rate. Specifically, in a range of low gas velocity, such as to guarantee a sufficient contact time, an enhancement of combustion stability is expected by increasing flow rate. Actually, an increase in the system adiabaticity is effective in preventing extinction, as it has been already shown [17,29]. Nevertheless, in a range of gas velocity not more compatible with the total fuel conversion, an increase in flow rate is detrimental for combustion stability causing blowout.

By analyzing the thermal profiles reported in Fig. 5, from 40 to 120 slph a maximum temperature is detected in correspondence with the middle of the reactor. Such a maximum increases by increasing the flow rate confirming the enhanced adiabaticity of the system. Moreover, the increase in the flow rate in the specified range brings about an increase in the fuel conversion (not reported) despite of the decrease of contact time, due to the faster catalytic combustion kinetics consequent to the increased temperature and to the higher mass transfer coefficient. The dynamics of quenching via extinction has been already discussed and pointed out in Fig. 4 at 80 slph. Such a behavior confirms that combustion stability in such range of flow rates is not limited by fuel conversion but only depends on heat losses.

Nevertheless, the worsening in stability observed by further increasing flow rate from 120 to 140 slph points out a changing in the combustion quenching mode from extinction to blowout. Under these conditions, the increase in the gas velocity brings about a decrease in the residence time in the high temperature zone, due to the drift of the heat wave downstream, as suggested



**Fig. 5.** QT of CH<sub>4</sub> at different the flow rates (■: 40 slph; △: 80 slph; ◆: 120 slph; ○: 140 slph) and fixed fuel concentration (Mix1). Temperature measured in the high conversion branch ((a)  $T_1$ ; (b)  $T_2$ ; (c)  $T_3$ ) as a function of the pre-heating temperature.

by the inversion of  $T_2$  and  $T_3$  values (i.e.  $T_3$  becomes higher than  $T_2$ ), with a displacement of the reaction front downstream.

The effect of the equivalence ratio on quenching has been studied changing fuel concentration and is reported in Fig. 6. On noble metals the increased equivalence ratio corresponds to enlarged operation windows [17]. Quenching temperature of Mix2 monotonically decreases with increasing flow rate from 40 to 120 slph down to near ambient temperature and results lower than the corresponding value of Mix1, thus extending the limits of stable combustion. It is worth noting that when external pre-

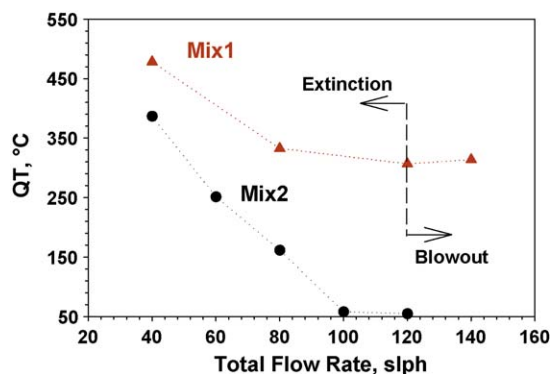


**Fig. 6.** QT of CH<sub>4</sub> at different flow rates and fuel compositions.

heating is too low it is technically difficult to control set-point temperature of the oven; as a result, critical temperature measurements are not reliable at the highest flow rate, thus suggesting us to avoid investigation at higher flow rates. The increased combustion stability is due to the higher temperature level developed inside the reactor and related to the higher thermal power developed by the richest mixture. By analyzing the trend of Mix2 quenching temperature with the flow rate, its decrease shows a tendency to level off at the highest investigated flow rates. Such a behavior may suggest a transition from an extinction to a blowout quenching regime further increasing the flow rate from 120 slph. If so, the use of richer mixture enlarged the operability limits in terms of pre-heating temperatures, but not in terms of flow rates, quenched via blowout occurring at roughly the same flow rate independently on the fuel mixture equivalence ratio. It is worth noting that quenching phenomena are strongly related to heat losses and, as a consequence, values of pre-heating temperature, equivalence ratio and flow rate corresponding to extinction/blowout are strictly related to the heat exchange with the surroundings, as reported by Zhong and Jiao [31].

### 3.2. Methane–hydrogen mixture ignition and quenching

In Fig. 7 the ignition transient of Mix3 at its MIT is reported. The experiment has been carried out at the same flow rate,  $Q_{TOT} = 80$  slph, considered in the Mix1 ignition test. In particular, thermal profile inside the monolith (Fig. 7a) as well as CH<sub>4</sub> and H<sub>2</sub> conversion measurements (Fig. 7b) are reported as a function of time. As shown for the light-off of Mix1 (Fig. 3), in Fig. 7 it is possible to distinguish four regions in the graph, Zones 1–4. Zone 5 corresponds to stable operation suspending CH<sub>4</sub> feeding, i.e. feeding Mix4. MIT measured under CH<sub>4</sub>–H<sub>2</sub> co-feeding is 450 °C, approximately 80 °C lower than that obtained in the case of Mix1 combustion. As a result, by substituting part of CH<sub>4</sub> with H<sub>2</sub>, maintaining the same input power to the reactor, enhances the fuel

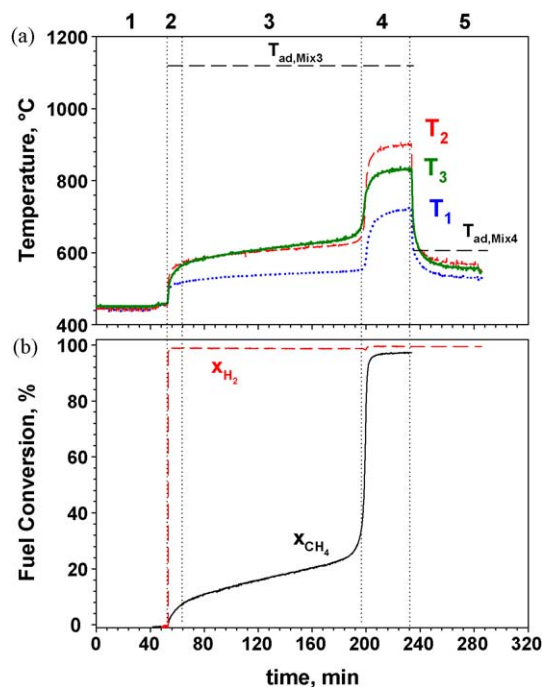


**Fig. 7.** CH<sub>4</sub>–H<sub>2</sub> MIT evaluation. Experimental conditions:  $Q_{TOT} = 80$  slph; Mix3 and Mix4. Section 1: thermal profile for an O<sub>2</sub>–N<sub>2</sub> mixture. Sections 2–4: CH<sub>4</sub> and H<sub>2</sub> are fed to the reactor: fuel light-off. Section 5: only H<sub>2</sub> is fed to the reactor. (a) Fuel conversions (CH<sub>4</sub>: solid line; H<sub>2</sub>: dashed line); (b) thermal profile inside the monolith ( $T_1$ : dotted line;  $T_2$ : dashed line;  $T_3$ : solid line).

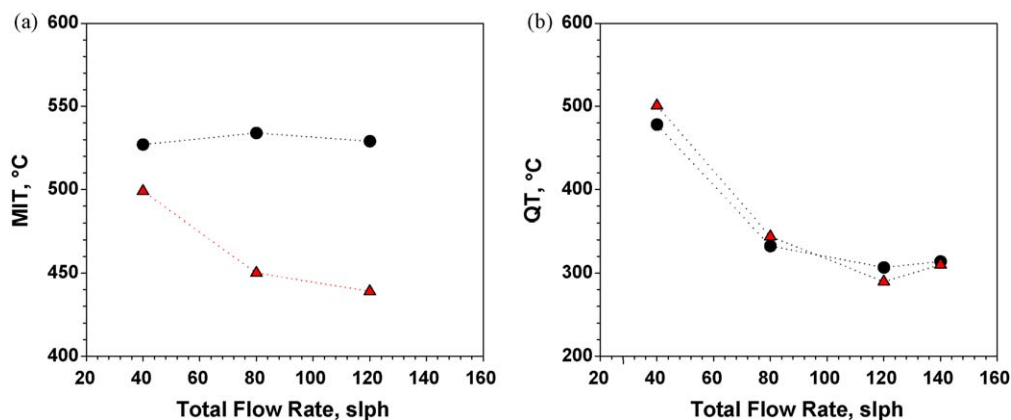


Fig. 8. MIT (a) and QT (b) of CH<sub>4</sub> (●) and CH<sub>4</sub>-H<sub>2</sub> (▲) combustion as a function of flow rate.

reactivity. It can be noted that, when fuel is fed to the reactor (Zone 2), hydrogen is totally converted due to the relatively high temperature and the presence of platinum in the catalyst, while CH<sub>4</sub> conversion is low (Fig. 7b). The heat developed by the combustion of H<sub>2</sub> produces an increase of the catalyst temperature to a level high enough to make starting the mechanism of heat accumulation and reaction rate rise already observed in Fig. 3 for CH<sub>4</sub> ignition (Zone 3), but in this case the phenomenon appears slower, induction time for light-off (Zone 4) being about 2 h, due to the lower temperature of surroundings (lower pre-heating temperature). The above results strongly suggest that H<sub>2</sub> and CH<sub>4</sub> combustions occurs separately during ignition, the former in the first part of the reactor, the latter downstream. As reported by Chao et al. [32], during ignition, i.e. at relatively low temperature, H<sub>2</sub>-CH<sub>4</sub> co-feeding does not influence hydrogen combustion on Pt sites, due to the preferential adsorption of H<sub>2</sub> on the noble metal. As a consequence, in our experiments on bi-functional Pt-LaMnO<sub>3</sub> catalyst hydrogen is totally burnt on Pt sites and shows a totally developed reaction front that, as it is expected, is placed in the middle part of the reactor. On the contrary, in Zones 2 and 3 methane combustion proceeds very slowly and is responsible for a gradual temperature increase at the exit of the reactor. As a consequence, the increased reactivity, i.e. the lower MIT, is due to a thermal more than chemical hydrogen assistance to methane combustion, related to the higher temperature level generated by H<sub>2</sub> combustion. Our results are in line with those obtained by Deutschmann et al. [37], who reported that H<sub>2</sub> addition to CH<sub>4</sub> reduces ignition temperature by providing catalyst temperature increase. This behavior has been also detected in a microcombustor [18], in the presence of significant heat losses.

When Mix4 is fed to the reactor (Zone 5), H<sub>2</sub> combustion contribution to heat release can be measured in terms of temperature increase with respect to temperature profile of Zone 1. Moreover, the thermal profile resulting in Mix4 combustion at a pre-heating temperature equals to Mix3 minimum ignition temperature, represents a sort of effective MIT of methane in CH<sub>4</sub>-H<sub>2</sub> mixture. Under these conditions  $T_3$  is about 550 °C, which is a value consistent with the minimum ignition temperature of methane measured on the same catalyst and at the same flow rate in absence of hydrogen (Fig. 3). The slight difference (about 30 °C) is due to the lower CH<sub>4</sub> partial pressure of Mix3 with respect to Mix1, corresponding to an higher light-off temperature. This behavior is generally due to the sticking tendency of methane and oxygen and occurs on Pt catalysts too [32].

In Fig. 8a MIT for Mix1 and Mix3 are reported as a function of the total flow rate. In the case of Mix1, MIT is practically independent on the flow rate in the limit of the experimental errors. Consistently with the value reported in the case of 80 slph,

MIT is around 530 °C in all the investigated cases, probably due to the dual effect of the flow rate on the fuel ignition: from one side by increasing the flow rate contact time decreases and as consequence fuel conversion decreases too, but on the other hand, by increasing the flow rate the thermal potential power increases too and, as a consequence, the developed power. According to the experimental results, these two effects are balanced and increasing the flow rate the same pre-heating temperature is required for ignition despite of the lower fuel conversion.

Differently from the case of methane combustion, MIT of CH<sub>4</sub>-H<sub>2</sub> fuel strongly depends on the flow rate, as it is shown in Fig. 8a, and, in particular, decreases increasing the flow rate, hydrogen addition resulting more and more effective. This behavior is related to the increased thermal power generated at high flow rate by hydrogen combustion, which is unaffected by contact time at the investigate temperatures, resulting in a higher and higher catalyst temperature increase due to H<sub>2</sub> combustion heat release.

On the contrary, no significant beneficial effect is detected on stability limits, i.e. on QT, as shown in Fig. 8b. This result strongly suggests that quenching phenomena are ruled by the ratio between the developed power via combustion and the power transferred to surroundings via heat losses, independently on the chemical composition of the fuel. As a matter of fact, once the fuel is ignited, the thermal balance, which regulates the self-sustainability of the reactor, exclusively depends on the ratio between the generated power and heat losses, both of them unaffected by fuel composition in our experiments, so explaining the undetectable effect of hydrogen addition on quenching temperature. This behavior is different from that observed on H<sub>2</sub>/CH<sub>4</sub> flames [38,39], where extinction phenomena strongly depend on the hydrogen-to-methane ratio. In fact, under homogeneous conditions H<sub>2</sub> co-feeding influences CH<sub>4</sub> combustion chemistry, while, as evidences before, under catalytic conditions H<sub>2</sub> effect is mainly thermal. This last consideration is more stringent if applied to Pt-LaMnO<sub>3</sub> catalyst, where the presence of two different sites provides the best active phases for H<sub>2</sub> (the noble metal) and CH<sub>4</sub> (the perovskite), as we previously observed [22].

#### 4. Conclusions

The auto-thermal combustion of methane and methane-hydrogen mixtures has been experimentally investigated by varying the gas flow rate, reactants concentration and composition and assessing the range of conditions in which a stable operation occurs. Under the experimental conditions investigated the heat supply from outside needed to ignite the combustion may be significantly reduced by partially substituting methane with hydrogen in the fuel. On the other hand, the system quenching

occurring with either extinction or blowout mechanism is not affected by fuel composition.

## References

- [1] R.E. Hayes, S.T. Kolaczowski, *Introduction to Catalytic Combustion*, Gordon and Beach Science Publishers, 1997.
- [2] C. Fernandez-Pello, *Proc. Combust. Inst.* 29 (2002) 883.
- [3] G.-G. Park, S.-D. Yim, Y.-G. Yoon, C.-S. Kim, D.-J. Seo, K. Eguchi, *Catal. Today* 110 (2005) 108.
- [4] G. Groppi, C. Cristiani, L. Lietti, P. Forzatti, *Stud. Surf. Sci. Catal.* 130D (2000) 3801.
- [5] D.G. Norton, D.G. Vlachos, *Proc. Combust. Inst.* 30 (2005) 2473.
- [6] S. Cimino, L. Lisi, R. Pirone, G. Russo, M. Turco, *Catal Today* 59 (2000) 19.
- [7] E. Arendt, A. Maione, A. Klisinska, O. Sanz, M. Montes, S. Suarez, J. Blanco, P. Ruiz, *Appl. Catal. A: Gen.* 339 (2008) 1.
- [8] D. Berger, C. Matei, F. Papa, D. Macovei, V. Fruth, J.P. Deloume, *J. Eur. Ceram. Soc.* 27 (2007) 4395.
- [9] G. Zou, L. Chen, X. Wang, *Catal. Lett.* 126 (2008) 96.
- [10] J.R. Paredes, E. Diaz, F.V. Diez, S. Ordonez, *Energy Fuels* 23 (2009) 86.
- [11] T. Asada, T. Kayama, H. Kusaba, H. Einaga, Y. Teraoka, *Catal. Today* 139 (2008) 37.
- [12] S. Cimino, A. Di Benedetto, R. Pirone, G. Russo, *Catal Today* 69 (2001) 95.
- [13] B. Kucharczyk, W. Tylus, *Catal. Lett.* 115 (2007) 122.
- [14] S. Cimino, R. Pirone, G. Russo, *Ind. Eng. Chem. Res.* 40 (2001) 80.
- [15] P.D. Ronney, *Combust. Flame* 135 (2003) 421.
- [16] D.G. Norton, D.G. Vlachos, *Combust. Flame* 138 (2004) 97.
- [17] N.S. Kaisare, S.R. Deshmukh, D.G. Vlachos, *Chem. Eng. Sci.* 63 (2008) 1098.
- [18] Y. Zhang, J. Zhou, W. Yang, M. Liu, K. Cen, *Int. J. Hydrogen Energy* 32 (2007) 1286.
- [19] O. Demoulin, I. Seunier, M. Navez, P. Ruiz, *Appl. Catal. A: Gen.* 300 (2006) 41.
- [20] O. Demoulin, I. Seunier, M. Navez, C. Poleunis, P. Bertrand, P. Ruiz, *Appl. Catal. A: Gen.* 310 (2006) 40.
- [21] A. Scarpa, R. Pirone, G. Russo, D. Vlachos, *Combust. Flame* 156 (2009) 947.
- [22] A. Scarpa, P.S. Barbato, G. Landi, R. Pirone, G. Russo, *Chem. Eng. J.* (2009), doi:10.1016/j.cej.2009.05.013.
- [23] S. Cimino, L. Lisi, R. Pirone, G. Russo, *Ind. Eng. Chem. Res.* 43 (2004) 6670.
- [24] E. Tzimpilis, N. Moschoudis, M. Stoukides, P. Bekiaroglou, *Appl. Catal. B: Environ.* 84 (2008) 607.
- [25] L. Giebler, D. Kießling, G. Wendt, *Chem. Eng. Technol.* 30 (2007) 889.
- [26] B. Kucharczyk, W. Tylus, *Catal Today* 90 (2004) 121.
- [27] M.J. Koponen, T. Venäläinen, M. Suvanto, K. Kallinen, T.-J.J. Kinnunen, M. Harkonen, T.A. Pakkanen, *Catal. Lett.* 111 (2006) 75.
- [28] S. Cimino, G. Landi, L. Lisi, G. Russo, *Catal. Today* 117 (2006) 454.
- [29] N.S. Kaisare, D.G. Vlachos, *Proc. Comb. Inst.* 31 (2007) 3293.
- [30] G. Veser, M. Ziauddin, L.D. Schmidt, *Catal Today* 47 (1999) 219.
- [31] B.-J. Zhong, J. Jiao, *Chem. Eng. Technol.* 31 (2008) 1342.
- [32] Y.-C. Chao, G.-B. Chen, H.-W. Hsu, *Catal. Today* 83 (2003) 97.
- [33] M. Maestri, A. Beretta, G. Groppi, E. Tronconi, P. Forzatti, *Catal. Today* 105 (2005) 709.
- [34] I. Aartun, B. Silberova, H. Venvik, P. Pfeifer, O. Görke, K. Schubert, A. Holmen, *Catal. Today* 105 (2005) 469.
- [35] A. Di Benedetto, S. Cimino, R. Pirone, G. Russo, *Catal. Today* 83 (2003) 171.
- [36] J. Li, H.G. Im, *Combust. Flame* 145 (2006) 390.
- [37] O. Deutschmann, L.I. Maier, U. Riedel, A.H. Stroemman, R.W. Dibble, *Catal. Today* 59 (2000) 141.
- [38] G.S. Jackson, R. Sai, J.M. Plaia, C.M. Boggs, K.T. Kiger, *Combust. Flame* 132 (2003) 503.
- [39] E.R. Hawkes, J.H. Chen, *Combust. Flame* 138 (2004) 242.